A Crystalline Catalyst Based on a Porous Metal-Organic Framework and 12-Tungstosilicic Acid: Particle Size Control by Hydrothermal Synthesis for the Formation of Dimethyl Ether

Da-Dong Liang,[a] Shu-Xia Liu,[a,*] Feng-Ji Ma,[a] Feng Wei,[a] and Ya-Guang Chen[a]

[a] Key Laboratory of Polyoxometalate Science of Ministry of Education, College of Chemistry, Northeast Normal University, Changchun, Jilin 130024, People's Republic of China
Fax: (+86)-431-8509-9328; e-mail: liusx@nenu.edu.cn

Supporting information for this article is available on the WWW under
http://dx.doi.org/10.1002/adsc.201000808.

Abstract: The strategy for obtaining a crystalline catalyst based on a porous copper-based metal-organic framework and 12-tungstosilicic acid with different particle sizes is reported. Through the control of hydrothermal synthesis and some simple treatments, catalyst samples with average particle diameters of 23, 105, and 450 μm, respectively, were prepared. This crystal catalyst has both the Brønsted acidity of 12-tungstosilicic acid and the Lewis acidity of the copper-based metal-organic framework, and has high density of accessible acid sites. Its catalytic activity was fully assessed in the dehydration of methanol to dimethyl ether. The effect of particle size on the catalytic activity of catalyst was studied, in order to select the particle size appropriate for avoiding the diffusion limitation in heterogeneous gas-phase catal-
ysis. In the selective dehydration of methanol to dimethyl ether, this catalyst exhibited higher catalytic activity than the copper-based metal-organic framework, γ-alumina, and γ-alumina-supported 12-tungstosilicic acid catalysts. It showed high catalytic performances, even at higher space velocity or in the presence of excess water. In addition, the catalyst was also preliminarily assessed in the formation of ethyl acetate from acetic acid and ethylene. It also exhibited a high activity which was comparable with that of silica-supported 12-tungstosilicic acid catalyst.

Keywords: dimethyl ether; ethyl acetate; heterogeneous catalysis; polyoxometalates; porous metal-organic frameworks

Introduction

At present, the scale of chemical production is enlarging each year to meet the rising demands for energy and chemical products. In order to reduce the corresponding economic and environmental pressure from the enlarged chemical production, we must develop novel environmentally benign catalysts with higher performances.

Polyoxometalates (POMs) and metal-organic frameworks (MOFs) are both environmentally benign catalytic materials. POMs, especially Keggin-type POMs, have attracted considerable research attention for a long time. The intrinsic chemical properties of Keggin-type POMs, such as strong Brønsted acidity and reversible oxidization properties, make them efficient catalysts in a large number of organic transformations and large-scale chemical production.[1] MOFs, consisting of metal ions or metal ion clusters and bridging organic ligands, are emerging porous materials. They combine well-defined crystalline structures, high surface areas, regular and tunable cavities, and high catalytic active site density. Their catalytic applications have caught the attention of researchers worldwide in recent years.[2]

Recently, hybrid compounds based on porous MOFs and POMs (PMOFs/POMs), which combine the properties of POMs and MOFs, have attracted special interest.[3] In the field of catalysis, several Keggin-type POMs have been dispersed in the porous systems of HKUST-1 [$Cu_3(BTC)_2(H_2O)_3$, BTC = 1,3,5-benzenetricarboxylate] and MIL-101 {$Cr_3F(H_2O)_2O$-[(O_2C)-C_6H_4-(CO_2)]$_3$}, respectively, and they exhibited high activities in some organic transformations.[4] Among them, only NENU-n series compounds have been well-defined by single-crystal X-ray diffraction.[4a] In NENU-n, each POM molecule is encapsulated in one pore of $Cu_3(BTC)_2$, resulting in the dispersion

of POMs molecules at the molecular level. The high pore density of $Cu_3(BTC)_2$ results in high POMs loading. The relatively narrow windows between the pores can physically prevent the agglomeration of POMs molecules and inhibit the leaching of POMs. In catalysis, the organic transformations may take place inside the porous system of the NENU-n. Each catalytically active site of NENU-n may be utilized, and the single-site catalysis leads to high catalytic activity.

In these NENU-n compounds, all catalytically active sites are located inside the porous system, and the internal diffusion limitation perhaps occurs in catalysis. An efficient method to avoid the diffusion limitation is to reduce the catalyst particle size. If the particle size is reduced, the reactant molecules will diffuse into the porous system at a higher speed, and the catalytic reaction will exhibit a higher rate. At the same time, each catalytically active site in the small particle where diffusion limitation is avoided may be utilized in the catalytic reactions. However, smaller is not always better. The smaller particle size brings more difficulties in the purification of catalysts and the catalytic operations. Thus, it is necessary to develop a synthesis method for controlling the particle size of NENU-n and to select the optimum particle size for each catalytic reaction. Hydrothermal synthesis is a universal method for synthesizing most PMOFs/POMs and all NENU-n compounds. It is safe and convenient, and the synthesis conditions can be easily controlled.

Herein, we obtained the $[Cu_2(BTC)_{4/3}(H_2O)_2]_6[H_2SiW_{12}O_{40}]\cdot(C_4H_{12}N)_2$ (NENU-1) with different particle sizes, through controlling the hydrothermal synthesis conditions. Then, $C_4H_{12}N^+$ cations

and H_2O were eliminated, and the resulting $[Cu_2(BTC)_{4/3}]_6[H_4SiW_{12}O_{40}]$ (NENU-1a) was used as the solid acid catalyst in the heterogeneous gas-phase catalysis of methanol dehydration to dimethyl ether (DME) and the formation of ethyl acetate from acetic acid and ethylene (Figure 1). Through comparing the catalytic activities of NENU-1a with different particle sizes, we selected the particle size appropriate for avoiding the diffusion limitation. In addition, the catalytic performances of NENU-1a were compared with those of the catalysts used in the present large-scale chemical production.

Results and Discussion

Catalyst Preparation and Characterization

NENU-1 was synthesized in a one-step hydrothermal reaction. The synthesis of NENU-1 to generate crystals that are suitable for single-crystal X-ray diffraction study has already been reported (CCDC 686793).[4a] Herein, the originally reported synthesis process has been modified to obtain NENU-1 with different particle sizes.

Through numerous synthesis experiments, we found that the final particle sizes of NENU-1 depend on the concentrations of reactants and the time of the hydrothermal reaction. Higher concentrations of reactants resulted in a higher nucleation rate and provided more nucleation sites that, in turn, facilitated the formation of a large number of small crystals. On the contrary, lower concentrations of reactants facilitated the formation of larger crystals, although the number of crystals was relatively small. The crystals were grown gradually under hydrothermal conditions, therefore, shortening the time of hydrothermal reactions resulted in small crystals and *vice versa*.

Crystalline samples of NENU-1 with average diameters of 23, 105, and 450 μm were obtained through applying different reactant concentrations and times of hydrothermal synthesis. Particle sizes were confirmed by SEM (Figure 2). The block-shaped crystals were isolated by centrifugation. Tiny differences in the shapes of the block-shaped crystals existed; however, these crystals had the same components and microstructures. The samples of NENU-1 were refluxed in ethanol and then treated at 180 °C under vacuum to remove $C_4H_{12}N^+$ and H_2O. Afterwards, NENU-1a samples were obtained.

The samples of NENU-1a with different particle sizes were identified by elemental analysis, IR, XRD, acid-base titration, and N_2 adsorption, respectively.

Elemental analysis indicates that, for these samples, the molar ratios of Cu:Si:W are all 12:1:12, which agrees with the reported molecular formula of NENU-1a.
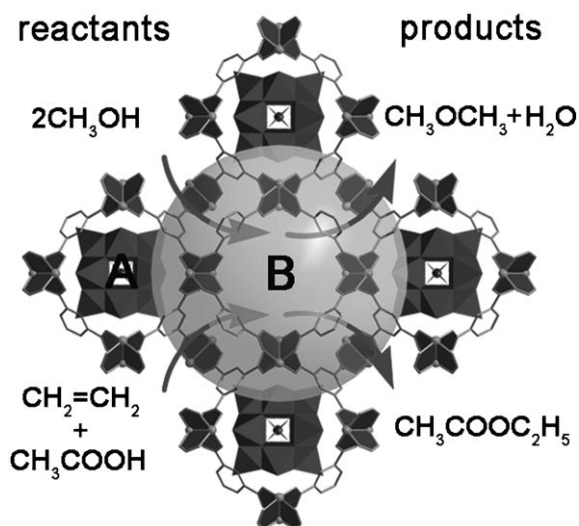

Figure 1. The catalytic dehydration of methanol to DME (*top*) and the formation of ethyl acetate from acetic acid and ethylene (*bottom*) were carried out in the porous system of NENU-1a.
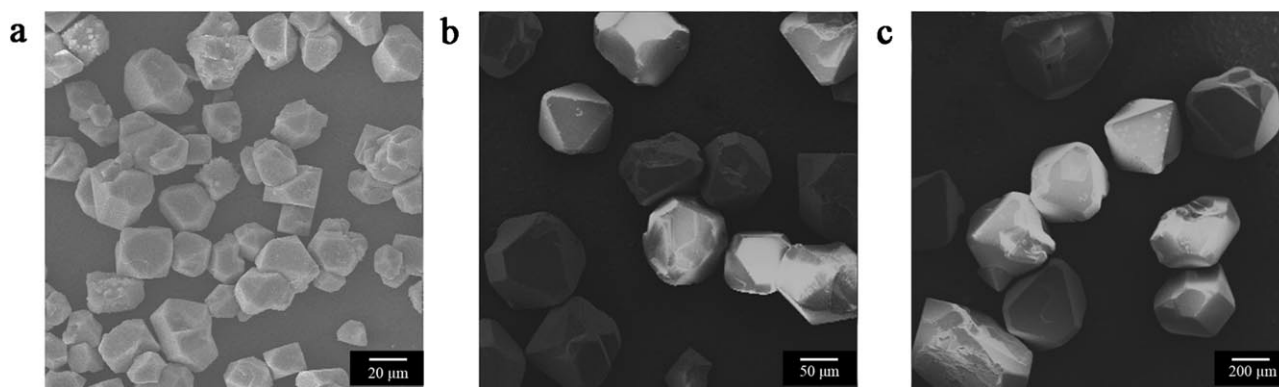
Figure 2. SEM of NENU-1 with average particle diameters of (**a**) 23, (**b**) 105, and (**c**) 450 μm.
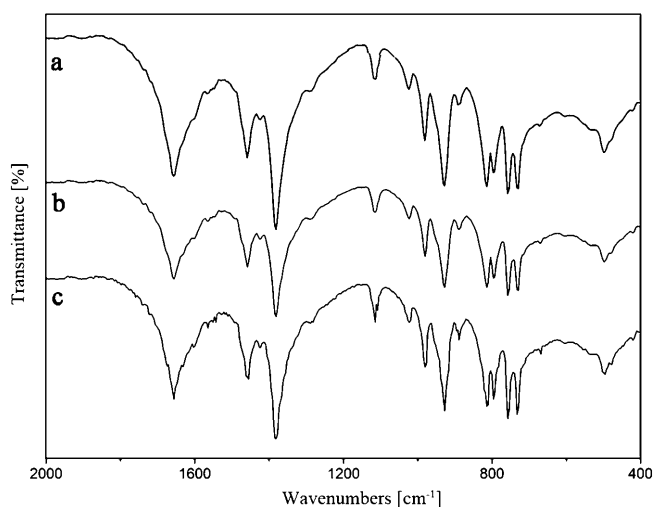

Figure 3. IR patterns of NENU-1a with average particle diameters of (**a**) 23, (**b**) 105, and (**c**) 450 μm.

The samples of NENU-1a with different particle sizes showed the same characteristics in the IR patterns (Figure 3), which indicates that they have the same components. The presence of Keggin-type 12-tungstosilicic acid and $Cu_3(BTC)_2$ in the samples of NENU-1a can also be confirmed through IR. As shown in Figure S1 in the Supporting Information, the main characteristic bands of $Cu_3(BTC)_2$ are in the range 1800–1090 cm^{-1} and 770–450 cm^{-1} region of the spectrum. The characteristic bands of $H_4SiW_{12}O_{40}$ are in the range 1020–770 cm^{-1}, and these bands are assigned to the vibration of $Si-O_a$, $W-O_{b/c}-W$, and $W-O_d$, respectively.[5] All of these characteristic bands of $Cu_3(BTC)_2$ and $H_4SiW_{12}O_{40}$ were observed in the IR pattern of NENU-1a, which demonstrates that 12-tungstosilicic acid and $Cu_3(BTC)_2$ are both present at the same time in NENU-1a. This conclusion may also be drawn through the comparison of IR patterns of NENU-1 and NENU-1a. Single-crystal X-ray diffraction of NENU-1 had unambiguously demonstrated the presence of Keggin-type POM in the porous

$Cu_3(BTC)_2$.[4a] The characteristic bands of NENU-1a, which are assigned to the $Cu_3(BTC)_2$ and 12-tungstosilicic acid, are in agreement with that of NENU-1 (see Figure S2 in the Supporting Information), which demonstrates that NENU-1a has the components of both $Cu_3(BTC)_2$ and 12-tungstosilicic acid. There is a tiny difference between the IR patterns of NENU-1 and NENU-1a. In the IR pattern of NENU-1a, a peak at 1484 cm^{-1} disappeared. This peak is assigned to the $C-H$ vibration. Its disappearance indicates that the $C_4H_{12}N^+$ cations had been decomposed through the vacuum heat treatment. After the decomposition of $C_4H_{12}N^+$ cation, H^+ was left on the polyanion, which could be confirmed through acid-base titration.[4a]

Acid-base titration results show that, in these samples, each $[SiW_{12}O_{40}]^{4-}$ corresponds to four protons. Taking the NENU-1a with the average particle diameter of 105 μm for example, in 0.5035 g NENU-1a, the proton amount is 0.38 mmol.

XRD patterns (Figure 4) of the NENU-1a bulk materials match the simulated pattern from the crystal structure of NENU-1, which indicates that the host structure of NENU-1 is maintained after the elimination of $C_4H_{12}N^+$ cations and H_2O, and that the NENU-1a samples have high purity. N_2 adsorption experiments indicate that all of these samples have high porosity. The representative adsorption isotherm of NENU-1a (particle diameter of 105 μm) is shown in Figure 5.

On the basis of the single-crystal X-ray diffraction study of NENU-1[4a] and the above characterization of NENU-1a, the structure of NENU-1a is confirmed. In NENU-1a, the MOF part is porous $Cu_3(BTC)_2$ which consists of paddle-wheel Cu_2 clusters and BTC groups. The $Cu_3(BTC)_2$ has two kinds of pores: A and B (see Figure 1). Pore A has a cuboctahedral shape. The BTC groups define 8 triangular planes of the cuboctahedra and the paddle-wheel Cu_2 clusters locate 12 vertices. Pore B is surrounded by 12 Cu_2 clusters and BTC ligands. In NENU-1a, each pore A accom-
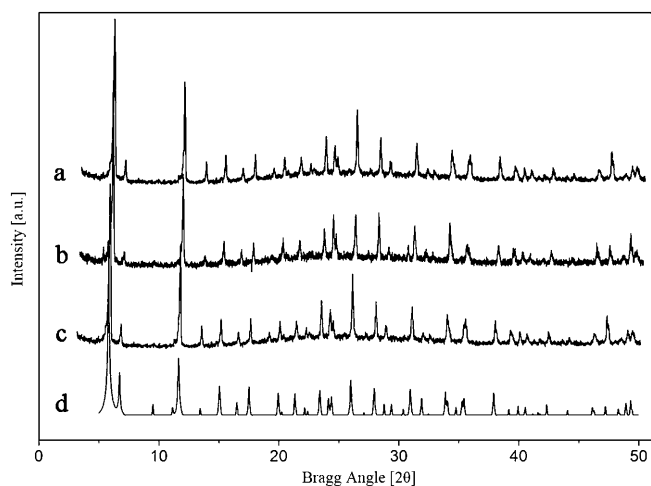
Figure 4. XRD patterns of NENU-1a with average particle diameters of (**a**) 23, (**b**) 105, and (**c**) 450 μm, and (**d**) XRD pattern simulated from the X-ray crystal structure of NENU-1 (CCDC 686793. These data can be obtained free of charge from The Cambridge Crystallographic Data Centre via www.ccdc.cam.ac.uk/data_request/cif).
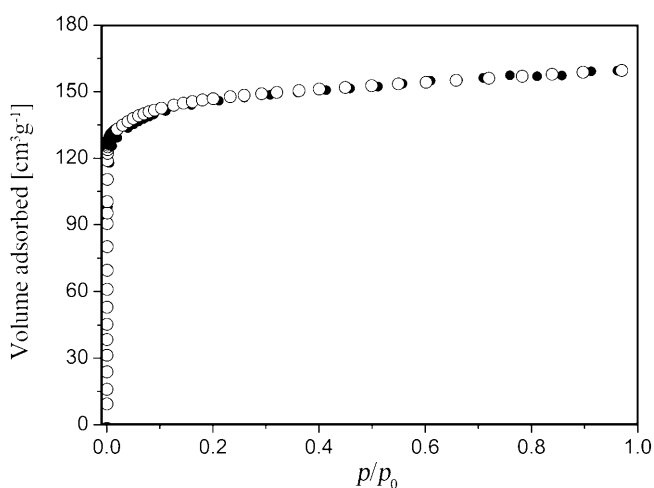

Figure 5. N_2 adsorption isotherm of NENU-1a (average particle diameter of 105 μm) measured at 77 K. Open symbols, adsorption; filled symbols, desorption.

modates one $H_4SiW_{12}O_{40}$ molecule, and all pores B are vacant. The diameter of pore B is 13 Å (see Figure S3 in the Supporting Information). These vacant pores B are connected to each other, and each pore B is connected to six adjacent pores B. Thus, NENU-1a exhibited high porosity.

The samples of NENU-n with different particle sizes have no difference in thermal stability. TG (Figure S4 in the Supporting Information) and variable-temperature XRD (Figure 6) show that NENU-1a is stable up to 300 °C, indicating that it has better thermal stability than pure $Cu_3(BTC)_2$ which is stable up to 240 °C.[6] The improved stability of the framework

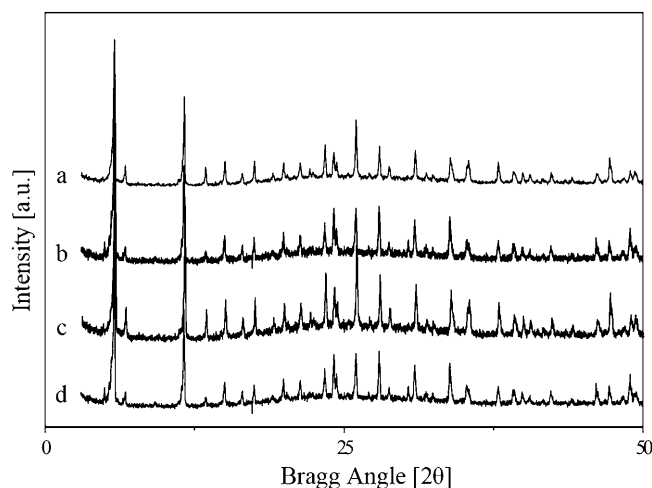**Figure 6.** XRD patterns of NENU-1a at different temperatures: (**a**) 240, (**b**) 260, (**c**) 280, and (**d**) 300 °C.

may be attributed to the POM encapsulation because the size, shape, and symmetry of $H_4SiW_{12}O_{40}$ highly match those of the pore A of $Cu_3(BTC)_2$. Because of such a molecular-level matching, Keggin-type POMs and Cu^{2+} ions of $Cu_3(BTC)_2$ may exhibit physico-chemical interaction.[31] Thus, when $H_4SiW_{12}O_{40}$ molecules are encapsulated in pores of $Cu_3(BTC)_2$, they can effectively support the framework and improve the stability.

Catalysis

The dehydration of methanol to DME was selected to assess the catalytic activity of NENU-1a. DME is a non-toxic, non-corrosive, non-carcinogenic, and environmentally-friendly chemical. It is a raw material for making important chemicals, including dimethyl sulfate and high-value oxygenated compounds. It is also used as an aerosol propellant in various spray cans, such as hair spray and shaving cream.[7] Furthermore, DME has been identified as a promising clean-burning alternative fuel. Its cetane rating is higher than that of conventional diesel fuel. It can be burned without the emission of soot, black smoke or SO_2, and only very low amounts of NO_x are produced.[8] Therefore, there is a growing requirement for the large-scale production of DME to meet the market. In China alone, there is more than one million tons of production capacity with another four million under construction.[9]

Selective dehydration of methanol, catalyzed by Brønsted acids and/or Lewis acids, is one of the common industrial methods employed for DME production. Although some homogeneous catalysts have been studied in recent years,[9] methanol dehydration to DME is mainly catalyzed over various solid-acid
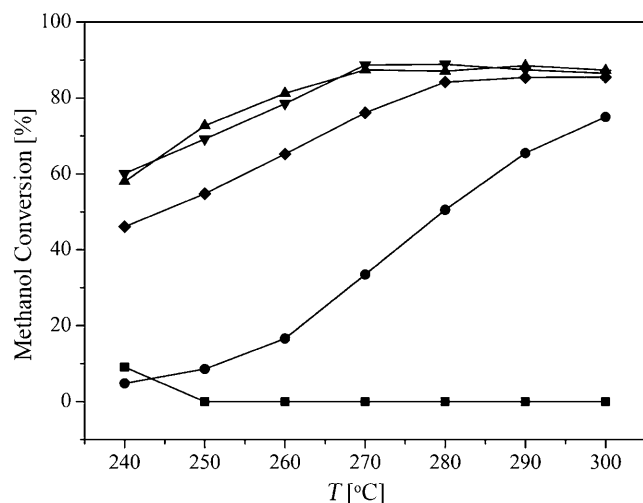
Figure 7. Conversions of methanol dehydration to DME over catalysts of (■) $Cu_3(BTC)_2$, (●) γ-Al_2O_3, and NENU-1a with the average particle diameters of (▼) 23, (▲) 105, and (♦) 450 μm at the pressure level of 0.6 MPa and LHSV of 2 h^{-1}.

catalysts,[10] because they are usually eco-friendly and can be separated easily from the reaction system. Developing novel solid-acid catalysts with better performances for the methanol dehydration to DME is being extensively pursued in both industrial and academic research.

The catalytic activity of NENU-1a in the heterogeneous gas-phase dehydration of methanol to DME was first compared with those of γ-Al_2O_3 and $Cu_3(BTC)_2$. γ-Al_2O_3 is a porous material with Lewis acidity and is commercially used for methanol dehydration to DME.[11] Pure $Cu_3(BTC)_2$ is also expected to catalyze methanol dehydration to DME because of its excellent Lewis acidity and high acid site density. In $Cu_3(BTC)_2$, all Cu are located in the paddle-wheel Cu_2 clusters. These coordinatively unsaturated metal centers are Lewis acid sites as proven in several works.[12]

The heterogeneous gas-phase catalyses of methanol dehydration to DME over γ-Al_2O_3, $Cu_3(BTC)_2$, and NENU-1a were performed in a fixed-bed reactor (Figure S5 in the Supporting Information) at a pressure level of 0.6 MPa and the liquid hourly space velocity (LHSV) of 2 h^{-1}. The respective performances of these catalysts are summarized in Table S1 in the Supporting Information and depicted in Figure 7. Over γ-Al_2O_3, the methanol conversion was 4.8% at 240°C; this gradually increased with increasing temperature. The conversion of methanol over $Cu_3(BTC)_2$ was 9.1% at 240°C, resulting in DME and water as the sole products. However, $Cu_3(BTC)_2$ is deactivated at higher temperatures due to the collapse of framework. These results indicate that although $Cu_3(BTC)_2$ is active and selective, methanol dehydra-

tion over $Cu_3(BTC)_2$ cannot achieve satisfactory conversion results by increasing the temperature.

Using NENU-1a as catalysts, DME selectivity reached 100% and methanol conversions were largely improved. At 240°C, methanol conversions over NENU-1a with average diameters of 23, 105, and 450 μm were 60.1%, 58.0%, and 46.1%, respectively. These values are higher than the 9.1% and 4.8% of methanol conversion over $Cu_3(BTC)_2$ and γ-Al_2O_3, respectively. From 250 to 300°C, NENU-1a still exhibited the highest activity among these three materials. The temperatures of equilibrium methanol conversion were 270, 270, and 280°C over NENU-1a, with average particle diameters of 23, 105, and 450 μm, respectively. These values are lower than that obtained over γ-Al_2O_3 (over 300°C), indicating that the DME production catalyzed by NENU-1a can be performed at a lower temperature than that catalyzed by γ-Al_2O_3. The pores in NENU-1a connect each other, and therefore the porous system is difficult to be blocked. In the long-term experiment of methanol dehydration, which was carried out on NENU-1a with the average diameter of 105 μm at 270°C, the conversions of methanol were almost constant over 168 h.

In the catalytic dehydration of methanol, NENU-1a with the average particle diameter of 450 μm exhibited lower activity than the samples with smaller particle diameters (23 and 105 μm), possibly due to internal diffusion limitation. In addition, in the NENU-1a with particle diameter of 450 μm, the active sites located in the deep pores of particles perhaps were not fully utilized. Methanol conversions over NENU-1a with average particle diameters of 23 and 105 μm generated similar results; indicating that the diffusion limitation was avoided after the particle average diameter was reduced to 105 μm.

The higher catalytic performance of NENU-1a than $Cu_3(BTC)_2$ is attributed to the POM encapsulation. $H_4SiW_{12}O_{40}$ is an excellent Brønsted acid, and the encapsulation of $H_4SiW_{12}O_{40}$ increases the number of acid sites per unit volume. On the other hand, POM encapsulation improved the thermal stability of the framework, which allows the Lewis acid sites of Cu(II) to improve their catalytic performances by appropriately increasing the reaction temperature.

Compared with γ-Al_2O_3, which has solely Lewis acidity, NENU-1a has additional Brønsted acidity. To assess NENU-1a further, a series of γ-Al_2O_3-supported $H_4SiW_{12}O_{40}$ catalysts with different POM loadings was prepared through impregnation. The samples with $H_4SiW_{12}O_{40}$ loadings of about 5, 10, 15, 20, and 30 wt% are denoted as $H_4SiW_{12}O_{40}$ (n%)/γ-Al_2O_3, where n = 5, 10, 15, 20, and 30, respectively. The methanol dehydration over γ-Al_2O_3 and γ-Al_2O_3-supported $H_4SiW_{12}O_{40}$ exhibited different conversions (Figure 8 and Table S2 in the Supporting Information). When the $H_4SiW_{12}O_{40}$ loading is in the range of

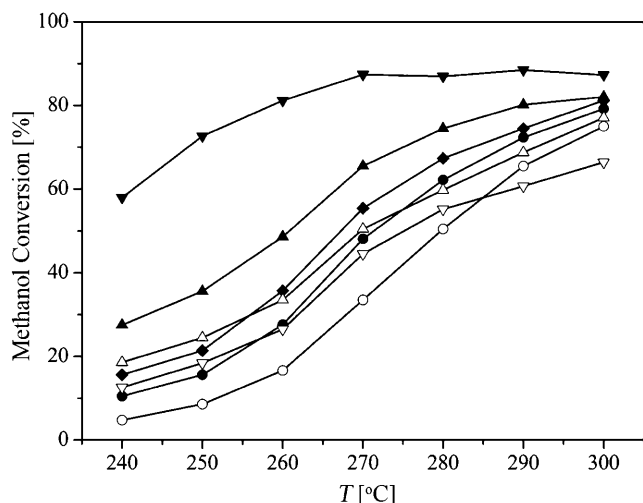**Figure 8.** Conversions of methanol dehydration to DME over (▼) NENU-1a with the average particle diameter of 105 μm, (○) γ-Al₂O₃, and γ-Al₂O₃-supported H₄SiW₁₂O₄₀ catalysts with the H₄SiW₁₂O₄₀ loading of (●) 5, (◆) 10, (▲) 15, (△) 20, and (▽) 30% at the pressure level of 0.6 MPa and LHSV of 2 h⁻¹.

Figure 9. Conversions of methanol dehydration to DME over catalysts of (▼) NENU-1a with average of 105 μm, (●) γ-Al₂O₃, and (◆) H₄SiW₁₂O₁₀ (15%)/γ-Al₂O₃ at the pressure level of 0.6 MPa and LHSV of 10 h⁻¹.

5% to 15%, the following sequence of catalytic activity has been observed: γ-Al$_2$O$_3$ < H$_4$SiW$_{12}$O$_{40}$ (5%)/γ-Al$_2$O$_3$ < H$_4$SiW$_{12}$O$_{40}$ (10%)/ γ-Al$_2$O$_3$ < H$_4$SiW$_{12}$O$_{40}$ (15%)/γ-Al$_2$O$_3$. This result indicates that the introduction of H$_4$SiW$_{12}$O$_{40}$ improves the catalytic performance of γ-Al$_2$O$_3$. With a POM loading higher than 15%, the sequence of catalytic activity is H$_4$SiW$_{12}$O$_{40}$ (15%)/γ-Al$_2$O$_3$ > H$_4$SiW$_{12}$O$_{40}$ (20%)/γ-Al$_2$O$_3$ > H$_4$SiW$_{12}$O$_{40}$ (30%)/γ-Al$_2$O$_3$. This indicates that excess POM in γ-Al$_2$O$_3$ may decrease the catalytic activity. When the H$_4$SiW$_{12}$O$_{40}$ loading is excessive, H$_4$SiW$_{12}$O$_{40}$ molecules are easily agglomerated by high surface energy, resulting in the partial blockage of the cavities of γ-Al$_2$O$_3$. Therefore, in order to obtain satisfactory conversion results, the H$_4$SiW$_{12}$O$_{40}$ loading over γ-Al$_2$O$_3$ must be limited at a reasonable level. Based on the results of the above experiments, the optimum POM loading should be set at 15%.

NENU-1a exhibited higher catalytic activity in comparison with various γ-Al$_2$O$_3$-supported H$_4$SiW$_{12}$O$_{40}$ catalysts (see Figure 8). Further comparison of the catalytic performance at higher LHSV demonstrates the apparent advantages of NENU-1a. The conversions over pure γ-Al$_2$O$_3$ and H$_4$SiW$_{12}$O$_{40}$ (15%)/γ-Al$_2$O$_3$ dramatically decreased at an LHSV of 10 h⁻¹, compared with the conversions at LHSV of 2 h⁻¹ (Figure 9 and Table S3 in the Supporting Information). In contrast, methanol dehydration over NENU-1a maintained high conversions. If NENU-1a is used to replace γ-Al$_2$O$_3$ or γ-Al$_2$O$_3$-supported H$_4$SiW$_{12}$O$_{40}$ as the catalyst in the production of DME, methanol dehydration may be performed at higher

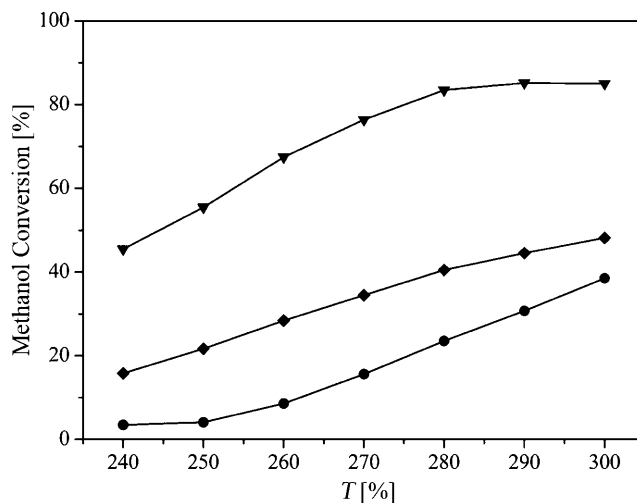LHSV, and more DME will be produced in any specific unit time.

The high catalytic performances of NENU-1a are associated with its structural features that not only allow high catalytic active site density, but also allow accessibility of all active sites. In NENU-1a, the H$_4$SiW$_{12}$O$_{40}$ loading (54 wt%) is much higher than the optimal loading (15 wt%) of γ-Al$_2$O$_3$-supported H$_4$SiW$_{12}$O$_{40}$ catalysts. Furthermore, all catalytic active sites in NENU-1a are accessible. Each H$_4$SiW$_{12}$O$_{40}$ with Brønsted acidity can access 6 vacant pores B through windows between pores A and B; each copper, which is a Lewis acid site, is located in the nodes of framework and points to the center of pore B (see Figure 1). Each catalytically active site in NENU-1a is freely accessible to reactant molecules, and the single-site catalysis ultimately results in high methanol conversion.

In this work, NENU-1a was also assessed in the catalytic dehydration of methanol in the presence of excess water. Water is one of the products of methanol dehydration, and the presence of excess water may decrease methanol conversion. In addition, water competes with methanol for the same Lewis acid sites on the catalyst, dramatically decreasing the Lewis acid activity.[7a] At 270°C, when the crude methanol with 20 wt% water was fed, methanol conversion over NENU-1a only slightly decreased, demonstrating the high water resistance of the NENU-1a (Figure 10). This result may be due to the high density of Brønsted acid sites of NENU-1a as supported by the fact that water only reduces the activity of Lewis acid sites but has little effect on Brønsted acid sites.[7a] As a result, when NENU-1a is used as the catalyst for DME production, cheaper crude methanol with a
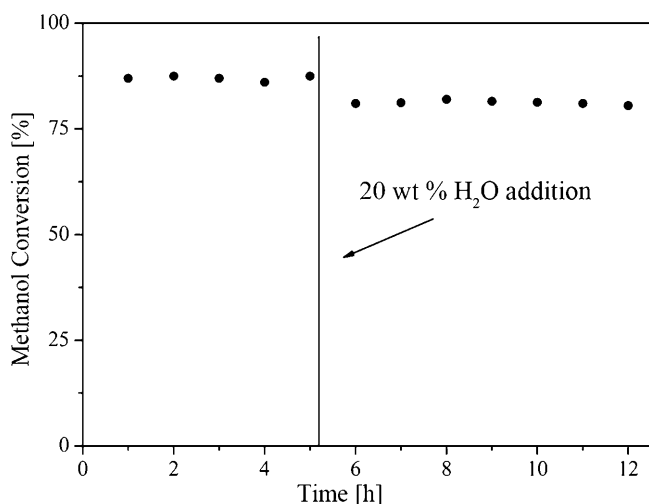
Figure 10. Water addition effect over NENU-1a. Anhydrous methanol was fed at the first 5 h, and then methanol with 20 wt% water was fed instead of anhydrous methanol. Conditions: 270 °C, 0.6 MPa, LHSV = 2 h^{-1}.

higher water content can be used as starting material instead of expensive anhydrous methanol. The high catalytic activity of NENU-1a in the presence of excess water also allows NENU-1a to be used in the syngas-to-DME process, which is another important industrial process involved in DME production.[13]

An important property of the PMOFs/POMs catalysts is that their catalytic performances may be fine-turned by encapsulating different POMs. A previous work has reported that NENU-3a [with $H_3PW_{12}O_{40}$ encapsulated in $Cu_3(BTC)_2$] showed high activity in the heterogeneous liquid-phase hydrolysis of esters.[4a] However, when NENU-3a was assessed in the catalysis of methanol dehydration, the highest selectivity of DME only reached 75%, which may be attributed to the strong acidity of $H_3PW_{12}O_{40}$. DME is an intermediate of methanol dehydration; if the acidity of the catalyst is too strong, the methanol tends to further dehydrate to form olefins or coke, thereby decreasing the selectivity of DME. $H_4SiW_{12}O_{40}$ has milder acidity and more protons than $H_3PW_{12}O_{40}$. Thus, NENU-1a is more suitable for catalyzing the selective conversion of methanol to DME than NENU-3a.

The mechanisms of catalytic methanol dehydration to DME differ over different solid acids.[14] In this work, an experiment of mixed alcohol dehydration was designed, and the mechanism of alcohol dehydration over NENU-1a was explored.

In the vapor adsorption experiments, NENU-1a adsorbed a large amount of methanol and only adsorbed a small amount of *n*-butanol (data not included in this work). Thus, NENU-1a may have the ability of adsorbing methanol selectively from the gas-phase mixtures of methanol and *n*-butanol.

The dehydration of mixed alcohols was performed in a modified fixed-bed reactor. The mixture, consisting of 10 atomic% methanol and 90 atomic% *n*-butanol, was introduced to the reaction zone by bubbling N$_2$ (99.999%) through a glass saturator filled with the mixture maintained at 25 °C. The effluent was monitored by GC.

When the reactor was at 25 °C, the content of methanol largely decreased once the alcohol solution passed through the reactor filled with NENU-1a, and no ethers were observed in the effluents. This phenomenon indicates that methanol molecules are selectively adsorbed on the surface of NENU-1a. They either coordinate to the copper of Cu$_2$ clusters or form hydrogen bonds with the POM molecules. The reaction of alcohol dehydration did not take place because of the low temperature.

The reactor was heated to 270 °C, and the dehydration reaction was carried out. In the production, *n*-butyl methyl ether was dominant and small amounts of DME and dibutyl ether were also present, as shown in Figure 11 and Table S4 in the Supporting Information. This can be explained in that the alcohol dehydration over NENU-1a is a surface reaction. One alcohol molecule is first adsorbed on the inner surface of NENU-1a, and a second alcohol molecule from the gas-phase interacts with the absorbed alcohol molecule. Methanol was the dominant adsorbed alcohol on the surface of NENU-1a; *n*-butanol is the dominant alcohol in the gas phase. Thus, *n*-butyl methyl ether is the main product. Because the contents of methanol and *n*-butanol are less in the gas phase and on the surface of NENU-1a, respectively, only less DME and dibutyl ether exist in the effluent.

NENU-1a was also assessed in the formation of ethyl acetate. Ethyl acetate is an important chemical product which is broadly employed as a solvent in paints, inks, enamels, adhesives, and the pharmaceuti-
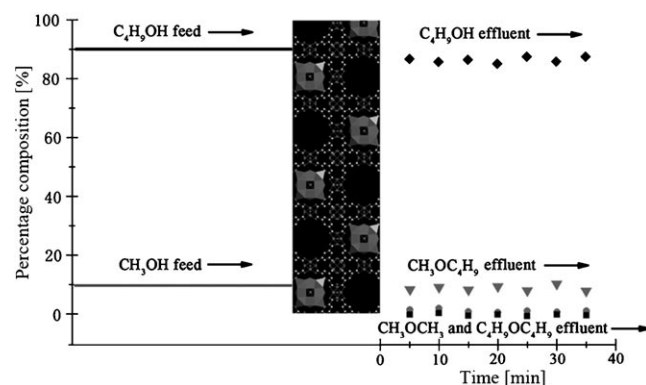

Figure 11. Dehydration of mixed alcohols, composed of 10% methanol and 90% butanol, over NENU-1a in a fixed-bed at 270 °C. The effluent consisting of (♦) C$_4$H$_9$OH, (▼) CH$_3$OC$_4$H$_9$, (●) CH$_3$OCH$_3$, and (■) C$_4$H$_9$OC$_4$H$_9$ was analyzed by GC every 5 min.

Table 1. Catalytic data for the formation of ethyl acetate from acetic acid and ethylene over various solid acid catalysts.

Entry	Catalyst	Yield of ethyl acetate [%]
1	H_3PO_4/SiO_2[a]	1[16]
2	Nafion-SiO_2[a]	3[16]
3	WO_3-ZrO_2[a]	0[16]
4	$H_4SiW_{12}O_{40}$[a]	0[16]
5	$H_4SiW_{12}O_{40}/SiO_2$[a]	50[16]
6	NENU-1a (450 µm)[b]	55
7	NENU-1a (105 µm)[b]	67
8	NENU-1a (23 µm)[b]	67

[a] *Reaction conditions:* reactant gas: acetic acid (8%), ethylene (78.5%), water (4.5%), and N_2 (9%); SV = 1500 h^{-1}, reaction temperature 438 K, and pressure 0.8 MPa.

[b] *Reaction conditions:* reactant gas, acetic acid (8%), ethylene (78.0%), water (5.0%), and N_2 (9%); SV = 1500 h^{-1}, reaction temperature 453 K, and pressure 1.0 MPa.

cal industry. It is a green alternative to aromatic compounds which cause serious damage to human beings and the environment.[15] The current annual demand of ethyl acetate approaches 1200 kilotons throughout the world, and the demand is still increasing each year.[16] The direct reaction of ethylene with acetic acid is one important industrial method for ethyl acetate production. SiO_2-supported $H_4SiW_{12}O_{40}$ catalyst is highly active for this reaction, and it has higher activity than H-montmorillonite, XE386 resin, nafion, H-zeolite Y, and H-theta-1.[17] Thus, it has been used in the present industrial ethyl acetate production.[18]

The activities of a section of solid-acid catalysts for the reaction of acetic acid with ethylene to form ethyl acetate are listed in Table 1, illustrating that NENU-1a is a highly active catalyst for this reaction. For NENU-1a, the selectivity of the ethyl acetate was more than 98%, while the activities were different, depending on the particle sizes. The sequence of yield is NENU-1a (450 µm) < NENU-1a (105 µm) = NENU-1a (23 µm). Thus, the NENU-1a with average particle diameter of 105 µm is the optimum for the catalytic reaction, because of the combination of high catalytic activity and appropriate particle size. In comparison with literature reports of the catalytic performances of catalysts should be treated with caution because of different experimental parameters.

Conclusions

The NENU-n series compounds are promising single-site catalysts. Their catalytic performances can be turned by encapsulating different POMs. The NENU-1a comprising $H_4SiW_{12}O_{40}$ is better than NENU-3a

comprising $H_3PW_{12}O_{40}$ for some selective acid catalytic reactions.

We have presented the particle size control of NENU-1 in hydrothermal synthesis for the catalytic applications. Through applying different reactant concentrations and hydrothermal synthesis times, we obtained the NENU-1 with the average particle diameters of 23, 105, and 450 µm, respectively.

NENU-1a has both the Brønsted acidity of $H_4SiW_{12}O_{40}$ and the Lewis acidity of $Cu_3(BTC)_2$, and it has a high density of accessible acid sites. Thus, it can be used as an effective single-site catalyst in acid catalysis. The internal diffusion limitation in the heterogeneous gas-phase catalysis was avoided, when the average particle diameter was reduced to 105 µm. In the catalytic dehydration of methanol to DME, NENU-1a exhibited higher catalytic performances than pure $Cu_3(BTC)_2$, γ-Al_2O_3, and γ-Al_2O_3-supported $H_4SiW_{12}O_{40}$ catalysts. If NENU-1a is used as the catalyst in the DME production, the catalytic reaction can be carried out at lower temperature, and the cheap methanol with high water content can be used as starting material instead of expensive anhydrous methanol. In addition, the study of mixed alcohols dehydration indicates that the dehydration takes place between the alcohol molecule adsorbed on the NENU-1a and a second alcohol molecule from the gas-phase. In the formation of ethyl acetate, the NENU-1a exhibited high catalytic activity, which was comparable with that of SiO_2-supported $H_4SiW_{12}O_{40}$ catalyst.

NENU-n series compounds are just the tip of the PMOFs/POMs iceberg. There are infinite possibilities for the combination of porous MOFs and POMs, especially when the diversity of the sizes and shapes of the MOFs cavities, as well as the diversity of the structures and components of POMs are considered. Continued engagement in the synthesis of PMOFs/POMs for catalytic applications will be encouraged in future work.

Experimental Section

Characterization Methods

Using KBr pellets, IR spectra were recorded in the range 400–4000 cm^{-1} on an Alpha Centaurt FT/IR spectrophotometer. XRD measurements were performed on a Rigaku D/MAX-3 instrument with Cu Kα radiation at 293 K. Element analysis was performed with a PLASMA-SPEC(I) ICP atomic emission spectrometer. Morphological characteristics of the samples were determined by scanning electron microscopy (SEM) using a Philips XL 30 microscope and a Shimadzu SSX-550 microscope. TG analysis was performed on a Perkin–Elmer TGA7 instrument in N_2 with a heating rate of 10 °C min^{-1}. The products of the catalytic experiments were analyzed with a GC (Agilent 6890N instru-

ment). Hiden Isochema Intelligent Gravimetric Analyser (IGA-100) was used to measure N_2 sorption; the NENU-1a sample (85 ± 1 mg) was used for the gas sorption measurement at 77 K.

Acid-base titration and back titration: Crystalline solid NENU-1a (0.5035 g) was placed in carbonate-free, sodium hydroxide solution (50.00 mL, 0.0125 M), which was standardized by titration with a standard potassium hydrogen phthalate solution. The mixture was sealed and stirred for 10 h at 25°C, filtering off the solids. Afterwards, the filtrate was back-titrated using hydrochloric acid (0.0118 M) standardized by titrations with the standardized sodium hydroxide solution. The number of acidic protons of NENU-1a was calculated from the amount of consumed sodium hydroxide.

Materials

Experimental $H_4SiW_{12}O_{40}$ and $Cu_3(BTC)_2$ were synthesized based on the procedures described in the literature;[19,12a] they were identified by IR and XRD. Other chemicals including those used for catalytic application were commercially purchased and used directly without additional purification.

$[Cu_2(BTC)_{4/3}(H_2O)_2]_6[H_2SiW_{12}O_{40}]\cdot(C_4H_{12}N)_2$ (NENU-1)

Preparation of a sample with an average particle diameter of 23 μm: A mixture of $Cu(NO_3)_2\cdot3H_2O$ (0.97 g, 4.0 mmol) and $H_4SiW_{12}O_{40}$ (0.80 g, 0.28 mmol) in distilled water (10 mL) was stirred for 15 min, after which H_3BTC (0.84 g, 4.0 mmol) and $C_4H_{12}NCl$ (0.44 g, 4.0 mmol) were added in succession. The pH of mixture was adjusted to 2–3 using $C_4H_{12}NOH$. After stirring for 2 h, the mixture was sealed in a Teflon-lined autoclave and heated at 180°C for 6 h followed by rapid cooling to room temperature. The crystallites of NENU-1 were separated from the mixture with a yield of 45% based on Cu.

Preparation of a sample with an average particle diameter of 105 μm: A mixture of $Cu(NO_3)_2\cdot3H_2O$ (0.48 g, 2.0 mmol) and $H_4SiW_{12}O_{40}$ (0.40 g, 0.14 mmol) in distilled water (10 mL) was stirred for 15 min, after which H_3BTC (0.42 g, 2.0 mmol) and $C_4H_{12}NCl$ (0.22 g, 2.0 mmol) were added in succession. The pH of the mixture was adjusted to 2–3 using $C_4H_{12}NOH$. After stirring for 2 h, it was sealed in a Teflon-lined autoclave and heated at 180°C for 15 h followed by rapid cooling at room temperature. The crystallites of NENU-1 were separated from the mixture with a yield of 60% based on Cu.

Preparation of a sample with an average particle diameter of 450 μm: A mixture of $Cu(NO_3)_2\cdot3H_2O$ (0.12 g, 0.5 mmol) and $H_4SiW_{12}O_{40}$ (0.10 g, 0.035 mmol) in distilled water (10 mL) was stirred for 15 min, after which H_3BTC (0.11 g, 0.5 mmol) and $C_4H_{12}NCl$ (0.055 g, 0.5 mmol) were added in succession. The pH of the mixture was adjusted to 2–3 with $C_4H_{12}NOH$. After stirring for 1 h, it was sealed in a Teflon-lined autoclave and heated at 180°C for 72 h followed by rapid cooling at room temperature. The crystallites of NENU-1 were separated from the mixture with a yield of 65% based on Cu.

$[Cu_2(BTC)_{4/3}]_6[H_4SiW_{12}O_{40}]$ (NENU-1a)

All the crystals of NENU-1 produced from the processes described above were refluxed in ethanol and then treated at 180°C under vacuum for 12 h to remove $C_4H_{12}N^+$ and H_2O. Afterwards, NENU-1a samples were obtained.

Catalytic Studies

A fixed-bed reactor was used to perform the heterogeneous gas-phase catalysis of methanol dehydration to DME and the formation of ethyl acetate from acetic acid and ethylene. The catalyst (NENU-1a) was packed in a steel reactor (inner diameter = 0.8 cm, length = 40 cm). Quartz wool was placed on the top and the base of the bed. The gas flow rate was controlled by a mass flow controller. Liquid was fed into the reactor by an ISCO liquid pump. In the catalytic dehydration of methanol, N_2 was used as a carrier gas, and the pressure drop over the reactor was 0.6 MPa. In the formation of ethyl acetate, the pressure is 1.0 MPa. The products were analyzed with GC.

In the study of the mechanism of alcohol dehydration, the reaction was performed in a modified fixed-bed reactor. The mixture, consisting of 10 atomic% methanol and 90 atomic% *n*-butanol, was introduced to the reaction zone by bubbling N_2 (99.999%) through a glass saturator filled with the mixture maintained at 25°C. The effluent was monitored by GC.

Supporting Information

The preparation of γ-Al_2O_3-supported $H_4SiW_{12}O_{40}$ catalysts, confirmation of the pore diameter in NENU-1a, IR of NENU-1a compared to that of $Cu_3(BTC)_2$, $H_4SiW_{12}O_{40}$, and NENU-1, TG analysis curve of NENU-1a, schematic view of experimental equipment, and tables of results of the catalytic transformations are available as Supporting Information.

Acknowledgements

References

[1] a) M. T. Pope, A. Müller, *Angew. Chem.* **1991**, *103*, 56–70; *Angew. Chem. Int. Ed. Engl.* **1991**, *30*, 34–48; b) N. Mizuno, M. Misono, *Chem. Rev.* **1998**, *98*, 199–218; c) I. V. Kozhevnikov, *Chem. Rev.* **1998**, *98*, 171–198; d) C. L. Hill, in: *Comprehensive Coordination Chemistry II*, Vol. 4, (Ed.: A. G. Wedd), Elsevier, **2004**, pp 679–759; e) *Polyoxometalates in Catalysis*, (Ed.: C. L. Hill), *J. Mol. Catal. A: Chem.* **2007**, *262*, 1–242 (special issue); f) I. V. Kozhevnikov, in: *Catalysts for Fine Chemical Syntheses*, Vol. 2, *Catalysis by Polyoxometalates*, Wiley & Sons, Chichester, England, **2002**,

pp 1–205; g) R. Neumann, A. M. Khenkin, *Chem. Commun.* **2006**, 2529–2538; h) R. Neumann, *Prog. Inorg. Chem.* **1998**, *47*, 317–370; i) A. M. Khenkin, G. Leitus, R. Neumann, *J. Am. Chem. Soc.* **2010**, *132*, 11446–11448; j) A. M. Khenkin, I. Efremenko, L. Weiner, J. M. L. Martin, R. Neumann, *Chem. Eur. J.* **2010**, *16*, 1356–1364; k) D. Baratsa, R. Neumanna, *Adv. Synth. Catal.* **2010**, *352*, 293–298; l) I. Boldini, G. Guillemot, A. Caselli, A. Proust, E. Galloa, *Adv. Synth. Catal.* **2010**, *352*, 2365–2370.

[2] a) G. Férey, C. Mellot-Draznieks, C. Serre, F. Millange, *Acc. Chem. Res.* **2005**, *38*, 217–225; b) G. Férey, *Chem. Soc. Rev.* **2008**, *37*, 191–214; c) L. Q. Ma, C. Abney, W. B. Lin, *Chem. Soc. Rev.* **2009**, *38*, 1248–1256.

[3] a) D. Hagrman, P. J. Hagrman, J. Zubieta, *Angew. Chem.* **1999**, *111*. 3359–3363; *Angew. Chem. Int. Ed.* **1999**, *38*, 3165–3168; b) L. M. Zheng, Y. S. Wang, X. Q. Wang, J. D. Korp, A. J. Jacobson, *Inorg. Chem.* **2001**, *40*, 1380–1385; c) C. Inman, J. M. Knaust, S. W. Keller, *Chem. Commun.* **2002**, 156–157; d) L. Yang, H. Naruke, T. Yamase, *Inorg. Chem. Commun.* **2003**, *6*, 1020–1024; e) G. Férey, C. Mellot-Draznieks, C. Serre, F. Millange, J. Dutour, S. Surblé, I. Margiolaki, *Science* **2005**, *309*, 2040–2042; f) S. X. Liu, L. H. Xie, B. Gao, C. D. Zhang, C. Y. Sun, D. H. Li, Z. M. Su, *Chem. Commun.* **2005**, 5023–5025; g) M. L. Wei, C. He, W. J. Hua, C. Y. Duan, S. H. Li, Q. J. Meng, *J. Am. Chem. Soc.* **2006**, *128*, 13318–13319; h) C. D. Zhang, S. X. Liu, B. Gao, C. Y. Sun, L. H. Xie, M. Yu, J. Peng, *Polyhedron* **2007**, *26*, 1514–1522; i) X. Y. Zhao, D. D. Liang, S. X. Liu, C. Y. Sun, R. G. Cao, C. Y. Gao, Y. H. Ren, Z. M. Su, *Inorg. Chem.* **2008**, *47*, 7133–7138; j) R. M. Yu, X. F. Kuan, X. Y. Wu, C. Z. Lu, J. P. Donahue, *Coord. Chem. Rev.* **2009**, *253*, 2872–2890; k) G. Hundal, Y. K. Hwang, J. S. Chang, *Polyhedron* **2009**, *28*, 2450–2458; l) S. R. Bajpe, C. E. A. Kirschhock, A. Aerts, E. Breynaert, G. Absillis, T. N. Parac-Vogt, L. Giebeler, J. A. Martens, *Chem. Eur. J.* **2010**, *16*, 3926–3932; m) X. F. Kuang, X. Y. Wu, R. M. Yu, J. P. Donahue, J. S. Huang, C. Z. Lu, *Nat. Chem.* **2010**, *2*, 461–465; n) G. F. Hou, L. H. Bi, L. X. Wu, *Inorg. Chem.* **2010**, *49*, 6474–6483; o) F. J. Ma, S. X. Liu, D. D. Liang, G. J. Ren, C. D. Zhang, F. Wei, Z. M. Su, *Eur. J. Inorg. Chem.* **2010**, *24*, 3756–3761.

[4] a) C. Y. Sun, S. X. Liu, D. D. Liang, K. Z. Shao, Y. H. Ren, Z. M. Su, *J. Am. Chem. Soc.* **2009**, *131*, 1883–1888; b) N. V. Maksimchuk, M. N. Timofeeva, M. S. Melgunov, A. N. Shmakov, Y. A. Chesalov, D. N. Dybtsev, V. P. Fedin, O. A. Kholdeeva, *J. Catal.* **2008**, *257*, 315–323; c) J. J. Alcañiz, E. V. Ramos-Fernandez, U. Lafont, J. Gascon, F. Kapteijn, *J. Catal.* **2010**, *269*, 229–241.

[5] C. Rocchiccioli-Deltcheff, M. Fournier, R. Franck, R. Thouvenot, *Inorg. Chem.* **1983**, *22*, 207–216.

[6] S. S. Y. Chui, S. M. F. Lo, J. P. H. Charmant, A. G. Orpen, I. D. Williams, *Science* **1999**. *283*, 1148–1150.

[7] a) M. T. Xu, J. H. Lunsford, D. W. Goodman, A. Bhattacharya, *Appl. Catal. A: Gen.* **1997**, *149*, 289–301; b) F. S. Ramos, A. M. D. Farias, L. E. P. Borges, J. L. Monteiro, M. A. Fraga, E. F. Sousa-Aguiar, L. G. Appel, *Catal. Today* **2005**, *101*, 39–44.

[8] G. A. Olah, A. Goeppert, G. K. S. Prakash, in: *Beyond Oil and Gas: The Methanol Economy*, Wiley-VCH, Weinheim, **2006**, pp 183–186.

[9] M. P. Atkins, M. J. Earle, K. R. Seddon, M. Swadźba-Kwaśny, L. Vanoyec, *Chem. Commun.* **2010**, *46*, 1745–1747.

[10] a) F. Yaripour, F. Baghaei, I. Schmidt, J. Perregarrd, *Catal. Commun.* **2005**, *6*, 542–549; b) F. Yaripour, F. Baghaei, I. Schmide, J. Perregaard, *Catal. Commun.* **2005**, *6*, 147–152; c) J. C. Xia , D. S. Mao, B. Zhang, Q. L. Chen, Y. H. Zhang, Y. Tang. *Catal. Commun.* **2006**, *7*, 362–366; d) K. Lertjiamratn, P. Praserthdam, M. Arai, J. Panpranot, *Appl. Catal. A: Gen.* **2010**, *378*, 119–123; e) Y. H. Seo, E. A. Prasetyanto, N. Jiang, S. M. Oh, S. E. Park, *Microporous Mesoporous Mater.* **2010**, *128*, 108–114.

[11] J. Khom-in, P. Praserthdam, J. Panpranot, O. Mekasuwandumrong, *Catal. Commun.* **2008**, *9*, 1955–1958.

[12] a) L. Alaerts, E. Séguin, H. Poelman, F. Thibauldt-Starzyk, P. A. Jacobs, D. E. D. Vos, *Chem. Eur. J.* **2006**, *12*, 7353–7363; b) K. Schlichte, T. Kratzke, S. Kaskel, *Microporous Mesoporous Mater.* **2004**, *73*, 81–88; c) R. Q. Zou, H. Sakurai, S. Han, R. Q. Zhong, Q. Xu, *J. Am. Chem. Soc.* **2007**, *129*, 8402–8403.

[13] D. S. Mao, W. M. Yang, J. C. Xia, B. Zhang, Q. Y. Song, Q. L. Chen, *J. Catal.* **2005**, *230*, 140–149.

[14] a) S. R. Blaszkowski, R. A. van Santen, *J. Am. Chem. Soc.* **1996**, *118*, 5152–5153; b) L. Kubelková, J. Nováková, K. Nedomová, *J. Catal.* **1990**, *124*, 441–450; c) J. Bandiera, C. Naccache, *Appl. Catal.* **1991**, *69*, 139–148.

[15] P. C. Zonetti, J. Celnik, S. Letichevsky, A. B. Gaspar, L. G. Appel, *J. Mol. Catal. A: Chem.* **2011**, *334*, 29–34.

[16] Y. Yamamoto, S. Hatanaka, K. Tsuji, K. Tsuneyama, R. Ohnishi, H. Imai, Y. Kamiya, T. Okuhara, *Appl. Catal. A: Gen.* **2008**, *344*, 55–60.

[17] M. J. Howard, G. J. Sunley, A. D. Poole, R. J. Watt, B. K. Sharma, *Stud. Surf. Sci. Catal.* **1999**, *121*, 61–68.

[18] I. V. Kozhevnikov, in: *Catalysts for Fine Chemical Synthesis*, Vol. 2, *Catalysis by Polyoxometalates*, (translated by P. K. Tang, X. G. Li, S. R. Wang), Chemical Industry Press, Beijing, **2005**, pp 208–209.

[19] E. O. North, *Inorg. Synth.* **1939**, *1*, 129–131.